Characterization of Air Breathing Plasma Thrusters Fuelled by Atmospheric Mixtures Encountered in Earth Atmosphere at an Altitude of About 200 km

IEPC-2015-268／ISTS-2015-b-268

Presented at Joint Conference of 30th International Symposium on Space Technology and Science
34th International Electric Propulsion Conference and 6th Nano-satellite Symposium,
Hyogo-Kobe, Japan
July 4 – 10, 2015

Konstantinos Katsonis[1] and Chloe Berenguer[2]
DEDALOS Ltd., Vassilisis Olgas 128, 54645, Thessaloniki, Greece

José Gonzalez del Amo[3*]
European Space Agency, ESTEC, Keplerlaan 1, 2200 AG Noordwijk ZH, The Netherlands

Abstract: Global modeling is used here to characterize various types of electric plasma thrusters, fuelled mainly by the atmospheric remnants encountered in about 200 km Earth altitude. Ground experimental devices meant to simulate thrusters functioning in space conditions are addressed by this modeling. Considered feeding includes up to five species (O, N_2 , O_2 , N and Ar) and their mixtures.

Nomenclature

4CGM = Four Components Global Model
5CArGM = Five Components Global Model (including Ar)
$\varepsilon_{C,X}$ = Collisional energy loss of the electrons, colliding with species *X*
ξ_{TOT} = Total ionization percentage
ABET = Air Breathing Electric Thruster
ABIE = Air Breathing Ion Engine
A_{eff} = Area for effective losses
CDF = Concurrent Design Facility
C-RM = Collisional-Radiative Model
EP = Electric Propulsion
ESA = European Space Agency
ET = Electric Thruster
FD = Functioning Diagram
GIE = Grid Ion Engine
GM = Global Model
HET = Hall Effect Thruster
HHT = Helicon Hall Thruster
HPT = Helicon Plasma Thruster
ICP = Inductively Coupled Plasma
ISRU = *In Situ* Resources Utilization
k_j = Rate coefficient of the process *j*

[1] Director, DEDALOS Ltd., katsonis.dedalos@gmail.com.
[2] Project Manager, DEDALOS Ltd., berenguer.dedalos@gmail.com.
[3] Head of Electric Propulsion Section, TEC-MPE, jose.gonzalez.del.amo@esa.int.

L = Plasma length
LEO = Low Earth Orbit
met = Metastable component
n_e = Electron density
n_i = Density of the species i
n_{ions} = Total density of positive ions
n_{TOT} = Total plasma species density
OES = Optical Emission Spectroscopy
p = Pressure
PaBE = Particle Balance Equation
P_{abs} = Absorbed Power
PCC = Plasma Components Composition
PiC = Particle in Cell
PoBE = Power Balance Equation
Q_{TOT} = Total flow rate
R = Plasma radius
RAM-EP = RAM type Electric Propulsion
RIT = Radio-frequency Ionization Thruster
T_e = Electron temperature
T_{GAS} = Temperature of neutrals
TOF = Time of Flight
$u_{B,X+}$ = $(eT_e/M)^{1/2}$, Bohm velocity of the ion X^+
V = Discharge volume
X_{TOT} = Total density of species X including excited ones

I. Introduction

THE present study concerns characterization of Electric Thrusters (ET) for Earth satellites evolving in typical altitudes from 180 km to 240 km in Low Earth Orbits (LEO). Such satellites are of current interest, mainly for telecommunications and for Earth observation. In order to obtain a readily available hence cheaper propellant for fuelling LEO satellite thrusters and to increase their lifetime, a disruptive technology has been previously initiated[1] by European Space Agency (ESA) aiming to use the low pressure atmospheric remnants at this altitude as a propellant. Meant to counterbalance the drag encountered in this region, Air Breathing Electric Thrusters (ABET) constitute a very promising issue, allowing for considerable spacecraft lifetime extension. This conception is part of a wider *In Situ* Resources Utilization (ISRU) technology, aiming to use also propellants based e.g. on oxygen resources of the Moon and of the ample CO_2 resources of the Mars atmosphere.

To support ABET technology, we lately developed a Global Model (GM) allowing for studying nitrogen/oxygen mixtures[2]. A conveniently adapted version of it, the Four Components Global Model (4CGM) is used here to investigate the physico-chemical properties of atmospheric mixtures of interest to ABET, encountered in altitudes of 180 km up to 240 km. Four initial components, namely O, N_2 , O_2 and N, have been initially taken into account in percentages varying according to the expected solar and geomagnetic activities[3]. For most ABET devices, the atmospheric mixtures have first to be collected to an adequate recipient, where they will be stored in pressures much higher than the initial surrounding atmospheric one, which is expected to be only around 0.0013 mTorr in 180 km altitude in case of mean conditions of solar and geomagnetic activity[4]. Once inside the selected EP device, the propellant constitution and properties will be modified, notably according to the available power to absorb, a process which also greatly depends on the feeding. The chemical constitution and the energetic balance can be foreseen and advantageously monitored in all phases by means of the elaborated 4CGM used here, sufficiently detailed in order to encompass the main chemical, collisional and radiative processes and to allow for Optical Emission Spectroscopy (OES) diagnostics. GMs also provide the necessary support for erosion preview and for evaluation of experimental results related to erosion processes. This has been made possible by inclusion of the necessary atomic data of O and N species and of their ions, besides the molecular ones. Note that an advantage of using GMs is that they are converging much faster than other type of models, e.g. the frequently used Particle in Cell (PiC) codes. This allows for a real time monitoring of the thruster. Because of the use of Ar as a non reactive propellant gas in some beam devices and experimental ABETs, a dedicated five component model version (5CArGM) has been also developed. Interesting results obtained by this model are presented in Section IV.

Technology initiated by ESA[1] addressed experimental characterization of Hall Effect Thruster (HET) and of Radio-frequency Ionization Thruster (RIT) types. The present GM is meant to also foresee the needs of further technological developments and to improve the status of theory – experiment comparisons, especially for ABET devices. Standard diagrams of Plasma Component Composition (PCC) belonging to each Functioning Diagram (FD) are used throughout to obtain a better insight of the mechanisms of propellant collection and handling and to improve OES diagnostics pertaining to EP thrusters. FD and PCC describe together the real time plasma characteristics for the prevailing plasma chemical constitution and physical conditions of interest. FD and PCC diagrams have been previously used profitably in studies addressing various ET types fed by Ar [5], by N_2O and air components[6] and by CO_2 [7].

On the basis of our GM results, for an imposed feeding and various pressures, FDs give the plasma ionization percentage depending on the electron temperature and on the absorbed power. Detailed composition of the plasma varying with pressure from 1 mTorr to 3 mTorr is given by concomitant PCC diagrams, one for each selected absorbed power value. Further insight can be obtained by means of PCCs showing variation of the detailed composition of the plasma as a function of the absorbed power for one selected pressure, here of 1 mTorr. FD and PCC diagrams presented in Sections III and IV provide abundances of the plasma components for various absorbed powers, flow rates, feedings and pressures which are on the basis of the ABET characterization. Initial atmospheric mixtures are those expected to be encountered in 180 km altitude. However, much higher pressures, about three orders of magnitude, are to be addressed, if a collector and storage vessel are to be used. Note that attempts have been made to use modified ABET versions, functioning at very low propellant pressures[8].

Physicochemical processes treated in detail by 4CGM play a crucial role in ABET feed considerations. E.g. in LEO environment, although often the atomic oxygen is initially the most abundant component (about 50%), because of the important dissociation of N_2 in case of sufficiently high absorbed power, N abundance may become higher than this of O, with the N^+ and O^+ ions being the most important ions present, encountered practically in equal percentages in a few mTorr pressure[2]. Details will be described in Section III.

In the present paper, after a simplified description of the GM in Section II, we develop ABET analysis by 4CGM in Section III, addressing pressure and absorbed power variations and discussing the obtained results. In Section IV, an application of 5CArGM in the characterization of a standard Air Breathing Ion Engine (ABIE) fed by an O_2 / Ar mixture is presented and discussed. Finally, conclusions are presented in the last Section V.

II. Simplified description of the Global Model

A global (volume averaged) model is essentially composed of:

(i) A Power Balance Equation (PoBE) which first describes the energy losses per electron-ion pair created and relates the so absorbed power with the electron density for a given electron temperature. Energy loss mechanisms include also subsequent ionization of singly ionized species, which becomes important for lower pressures and higher temperatures. Energy losses from electronic or vibrational excitation must also be included. In the present case of interest, energy losses due to "chemical" processes and especially to molecular dissociation are also included. In so doing, losses coming from volume collisions of species and their flows to the walls are taken into account.

(ii) The Particle Balance Equations (PaBEs), a set of statistical equations corresponding to the studied discharge. Each equation corresponds to one of the species of which we calculate the populations, with their system describing the global kinetics of the present particles.

To describe the physical and chemical situation, it becomes necessary to resolve the set of equations (i) and (ii) under the effective form factor, together with additional adequate equations, describing the plasmas processes and overall discharge. Such additional equations have been used e.g. in the study of Ar fed arc-jet devices[9], where Navier-Stokes equations have been added to the set of equations (i) and (ii). Data from Collisional-Radiative Models (C-RMs), are used to write down the particle balance equations (PaBEs) of the GM. Such a model constitutes the basis of the thruster characterization and of a detailed plasma study based on the expected fuel constituents, also supporting Optical Emission Spectroscopy (OES) diagnostics and erosion assessment.

In case of a simplified steady-state solution the PoBE can be written as:

$$P_{abs}/V = \sum_{X} e\varepsilon_{C,X} k_{IONIZ,X} n_X n_e + \sum_{X+} e(\varepsilon_e + \varepsilon_i) k_{RW,X+} n_{X+} \tag{1}$$

where V is the discharge volume, P_{abs} is the power absorbed by the plasma and n_e is the electron density, with e the electron charge. The sum is made over all the ground level species whith a density n_X, a collisional energy loss term $\varepsilon_{C,X}$ and an ionization rate coefficient $k_{IONIZ,X}$. In the second term, $k_{RW,X+}$ is the wall recombination rate, given by

$k_{RW,X+} = u_{B,X+} \cdot A_{eff} / V$, where $u_{B,X+}$ is the Bohm velocity of the ion X^+ , $u_{B,X+} = (eT_e/M)^{1/2}$ with M the species mass and A_{eff} is the area for effective losses. Also, ε_i and ε_e represent the mean kinetic energy lost per ion and per electron respectively. To the PoBE equation (1) the PaBE set of equations (2) is added, of which each equation, say of species *j*, is constituted by the sum of all the creation and destruction terms for the given species *j* and can be written as:

$$\frac{dn_j}{dt} = \sum R^j_{Production} - \sum R^j_{Loss} \qquad (2)$$

where Σ denotes the sum of all terms including production $R^j_{Production}$ and loss R^j_{Loss} rates involving the species *j*. Each reaction rate is given by the product of the reactant densities n_i and the corresponding rate coefficient k_j :

$$R^j = k_j \cdot \prod_i n_i \qquad (\mathrm{cm^{-3}s^{-1}})$$

Following the described procedures, an argon GM[5], a N_2O and air GM (detailed description given previously[10]) and a CO_2 GM[7] have been developed and used in the study of electric thrusters fed by the most promising propellants.

As reported in the introduction, atmospheric data and exploitation of related feeding studies have been used to obtain results for the four most abundant species encountered in about 200 km altitude from sea level, O, N_2 , O_2 and N including their mixtures (4CGM model[2]). Comparison of our results with existing both theoretical and experimental ones allowed for validation of 4CGM, not only in numerous Inductively Coupled Plasma (ICP) reactors and glow discharges cases[10], but also for atmospheric remnants compositions evaluation[3] at altitudes from 180 km to 240 km. Especially for N_2 feeding, GMs allowed for a comparison with thrust measurements for HET and Grid Ion Engine (GIE) / RIT thrusters[11,12].

Including detailed data for N / N_2 and O / O_2 and of their compounds allows for obtaining realistic modeling for pure nitrogen and oxygen feeding and for their mixtures[12]. We remind that GM results were also systematically presented there[12] under the form of Functioning Diagrams (FD) giving the total ionization percentage of the plasma thruster for a selected flow rate value, followed by evaluation of Plasma Components Composition (PCC) for the investigated sets of physical conditions.

III. ABET analysis by 4CGM

The present section addresses general considerations on the characterization of electric plasma thrusters fed with atmospheric remnant propellant. This analysis provides first a general idea on how a plasma discharge composed of various atomic and molecular nitrogen and oxygen mixtures is reacting under pressure and power variations for a given flow rate. Important ABET parameters obtained by 4CGM are presented and commented. The FDs and PCCs obtained for the four main components of the atmosphere remnants are discussed in the following. Concomitant T_e and ξ_{TOT} variations are also discussed. Results are further compared with those obtained assuming pure atomic oxygen feeding[13].

The present 4CGM version takes into account the four initial components, O, N_2 , O_2 and N also including their atomic and molecular structures. These four components were selected because they are the main constituents in the Earth atmosphere at an altitude of about 200 km which is of interest in the present study[3,14]. Results obtained using the 4CGM model have been previously presented in a recent ESA Workshop[2].

A specific feeding of 50.1% O / 47.5% N_2 / 2.16% O_2 and 0.28% N is used here, which is expected to correspond to the atmospheric mixture composition found in a typical altitude of 180 km in case of mean solar and geomagnetic activity. To illustrate the importance of the considerable amount of N_2 presence in the propellant, results are compared with those obtained for molecular O_2 and for sole atomic oxygen O feeding in similar conditions. In the FDs presented here, the total ionization percentage $\xi_{TOT} = n_{ions} / n_{TOT}$ (%) is given as a function of pressure (*p*), for various absorbed power (P_{abs}) and electron temperature (T_e) values. Note that only the number of ions enters in ξ_{TOT} without including their ionization degree. The total charge is appreciated from the given n_e / n_{TOT} values. To a given FD correspond PCCs illustrating the variation of the density of species as a function of the pressure and the absorbed power. Hence, elaboration of such diagrams illustrates the variations of the plasma ionization and composition as a function of various parameters including feeding, pressure and absorbed power.

Selected parameters are those expected to correspond to typical air breathing thrusters. An unique form factor of *L* = 13 cm and *R* = 5 cm is used in the calculations. A typical feeding of 20 sccm is selected, but various feeding values for O_2 / N_2 mixtures can be considered[12]. The flow rate of 20 sccm is of the order of the propellant provided by a collector of 1 m^2 cross section area, flying at 8 km/s at an altitude of 180 km. Temperature of the neutrals was taken to be 853 K throughout. All figures concern exclusively the aforementioned parameters. Although in the present work we address only thrusters functioning in low pressures, going from 1 mTorr to 3 mTorr, higher pressure conditions have been also examined and they will be addressed elsewhere.

A. Importance of the thruster pressure

In Fig. 1 we present a typical PCC diagram for P_{abs} = 400 W absorbed power when pressure varies from 1 mTorr to 3 mTorr. The suffix TOT indicates the total values of various components, in case separate values of excitation / ionization are available. Fig. 1 shows n_{TOT} and n_e values, which are comparable at about 1 mTorr pressure, indicating a significant ionization, but differ by an order of magnitude for 3 mTorr. This indicates a low ionization for higher pressure, limited by the available P_{abs} of 400 W. Consequently, N^+ and O^+ become the prevailing species for low pressures in this case, although slightly diminishing with pressure. Other important presences are those of atomic nitrogen and oxygen, both strongly increasing with increasing pressure and in a similar way. Presences of the two atomic species and of their single ions are not very different for nitrogen and for oxygen. Notably, nitrogen atoms and their single ions are more present than oxygen ones, although about half of the propellant fed consists of N_2 .

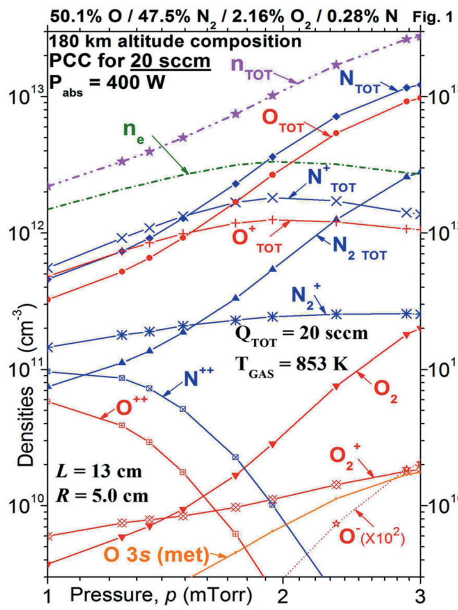

Figure 1. 400 W PCC.

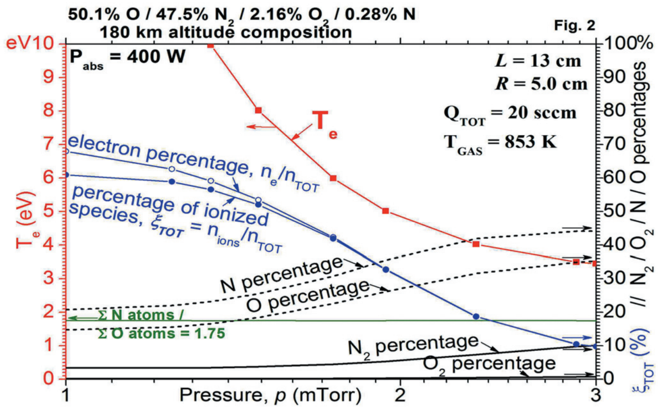

Figure 2. 400 W T_e , ξ_{TOT} , electron percentage and remaining N_2 , N, O_2 and O percentages.

We can see in Fig. 1 that N_2 and O_2 species densities are small for 1 mTorr but they increase very quickly with pressure. Molecular ions N_2^+ and O_2^+ have low densities which increase very slowly with pressure increase. For low pressures about 1 mTorr, the molecular ions are more present than the neutral molecules. For higher pressures, presence of the neutral molecules increases considerably, then becomes an order of magnitude higher than this of molecular ions in about 3 mTorr. It is important to notice that presence of nitrogen molecules and of their single ions vary in a similar way with this of the oxygen, but the former are at least about one order of magnitude higher.

The twice ionized species N^{++} and O^{++} represent nearly 10% of the total species for 1 mTorr, but their densities decrease sharply with pressure. O^- density is orders of magnitude lower, therefore is shown here multiplied by 100. Also, density of the oxygen metastable level, O 3*s* $^5S_2$ (represented with orange line), is increasing with pressure. Results change substantially within the 1 mTorr to 3 mTorr pressure domain. On the contrary to the O case, N and N^+ species have not clear metastable states, therefore all of their excited species populations are very low and O I lines are mostly expected to appear in the visible region. However, N_2 molecular spectra are expected to be more intense than those of O_2 .

Concomitant variations of the T_e , of ξ_{TOT} , of the electron percentage and of the remaining neutral species percentages are shown in Fig. 2. They also correspond to pressure variations from 1 mTorr to 3 mTorr and 400 W absorbed power. For low pressure, T_e becomes very high, but it has to be appreciated that it is difficult to obtain 400 W absorption by the propellant in such low pressures. Also, presence of energetic electrons leads to considerable multiple ionization, thus contributing to increase the absorbed energy losses.

In order to get a glimpse of the influence of the absorbed power important parameter, we present in Fig. 3 a PCC corresponding to a higher absorbed power of 1000 W. Although the main trends remain similar to those obtained for absorbed power of 400 W illustrated in Fig. 1, a significant increase of the ionized species densities is observed for the 1 kW case of Fig. 3 because of the high absorbed power.

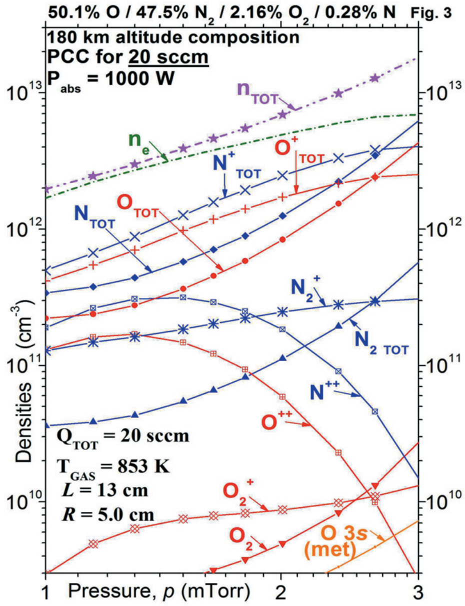

Figure 3. 1000 W PCC.

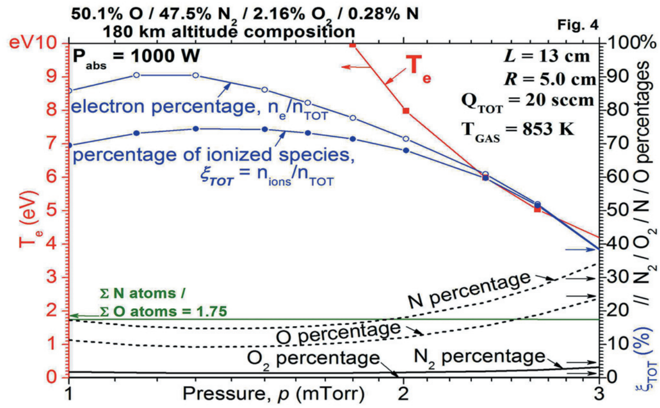

Figure 4. 1000 W T_e , ξ_{TOT} , electron percentage and remaining N_2 , N, O_2 and O percentages.

In Fig. 3, we observe that the twice ionized species vary in a totally different way than the singly ionized ones. Mind that higher ionized species are expected to appear in this region, which are not included in the figure.

The corresponding variations of the T_e , ξ_{TOT} , electron and remaining neutral species percentages are shown in Fig. 4. Evidently, higher ionization percentage and electron temperature are observed for the 1000 W case (Fig. 4) than for the 400 W one (Fig. 2). Thus, percentages of remaining neutral species N, O, N_2 and O_2 are quite smaller for 1000 W than in the 400 W case.

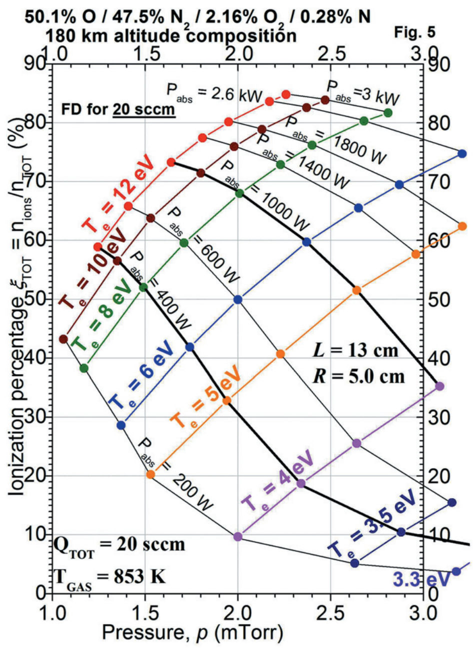

Figure 5. FD for an atmospheric mixture feeding of 20 sccm.

Using various PCCs corresponding to different absorbed power values, it is possible to construct a FD, which encompasses both pressure and power variations. Fig. 5 shows such a FD pertaining to GM results for the same atmospheric mixture feeding of 20 sccm. It illustrates ionization percentages variation as a function of pressure for a set of absorbed power and T_e values. Absorbed powers addressed span a range of 200 W to 3 kW and the T_e a range of 3.3 eV to 12 eV, for a limited variation of the pressure from 1 mTorr up to 3 mTorr. This FD encompasses a very wide range of plasma parameters, with the pressure remaining quite low. We insist on the fact that this standard FD is dedicated to a defined flow rate of 20 sccm. The two curves corresponding to the previously considered P_{abs} = 400 W and P_{abs} = 1 kW PCCs are shown with thick lines. The situation should be very different for different flow rates. Note that in the diagram of Fig. 5, a 10% limit of ion losses from the "core" plasma to the walls was fixed.

Variations of the plasma ionization for the investigated atmospheric mixture is clearly illustrated by the FD of Fig. 5. Specifically, we observe a considerable ionization when pressure is decreasing and/or power is increasing. In order to reveal the role of the N_2 presence, constituting about 50% of the number density in about 200 km, the obtained results for atmospheric mixtures are compared to those corresponding to pure atomic oxygen feeding. Results pertaining to oxygen are here obtained with the same 4CGM but supposing only atomic oxygen feeding. The bulk chemical composition change, but an important difference is here that the propellant feed is in atomic state, so no absorbed energy is spent to volume dissociation, as was the case with N_2 molecules. Thereafter, we present atomic oxygen feeding 4CGM results, for a quite high absorbed power.

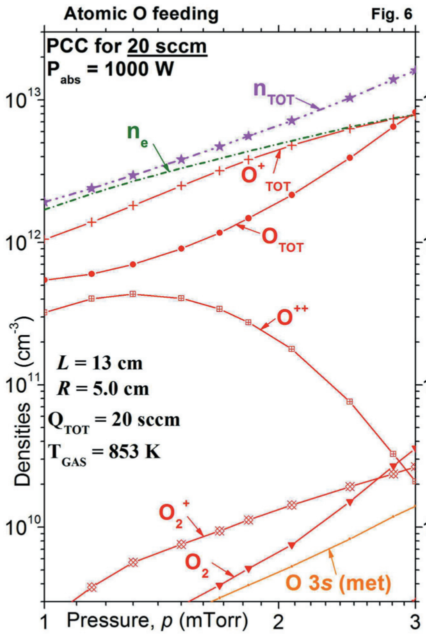

Figure 6. 1000 W PCC for atomic oxygen feeding.

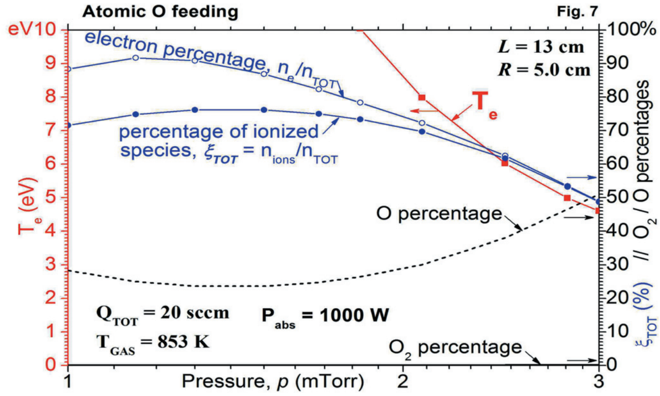

Figure 7. 1000 W T_e , ξ_{TOT} , electron percentage and O and remaining O_2 percentages.

The corresponding PCC diagram meant for 1000 W absorbed power and pressure varying from 1 mTorr to 3 mTorr is presented in Fig. 6. In this PCC, we observe that main species is O^+, especially for the lower pressures investigated and that molecular species have much lower densities which increase with pressure. The O^{++} ion presence is important, especially for pressures lower than 2 mTorr. Increase of the pressure to 3 mTorr suffices to increase neutral O presence to the O^+ level and to lower O^{++} presence of an order of magnitude with similar increase of molecular presence.

The corresponding variations of the T_e , the ξ_{TOT} , the electron percentage and the remaining neutral species percentages, are represented in Fig. 7 for the same atomic oxygen discharge with 1000 W absorbed power. We observe that, as expected, electron temperature, electron percentage and ionization percentage are quite high. It is

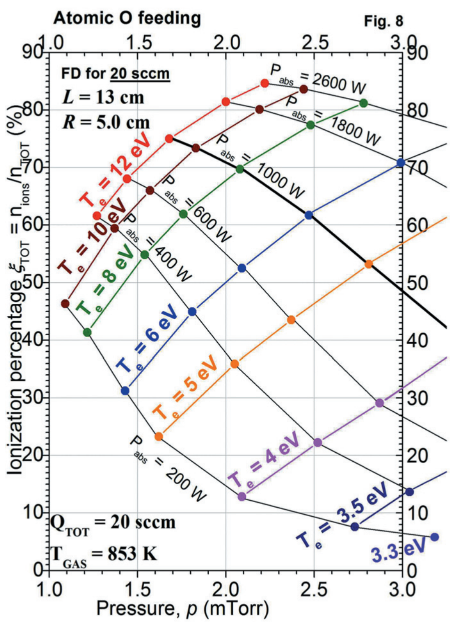

Figure 8. FD for 20 sccm atomic oxygen feeding.

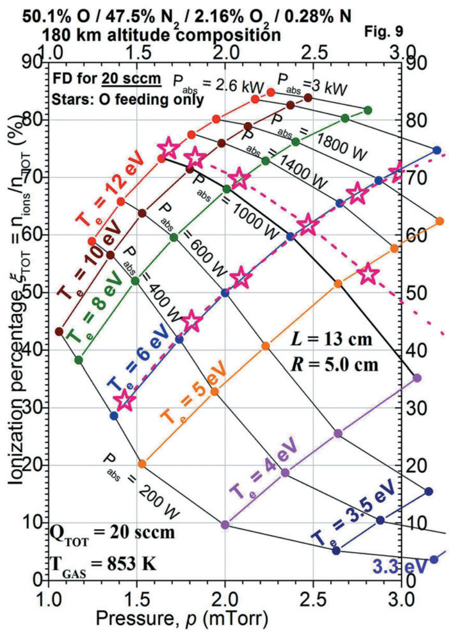

Figure 9. FD comparing atmospheric mixture and O (big pink stars) feedings.

important to note that when passing from the atmospheric mixture feeding (Fig. 4) to pure atomic oxygen one (Fig. 7), the ionization percentage shows a relative increase of up to 25%.

More generally, it is interesting to represent how the atomic oxygen discharge ionization is varying both as a function of the pressure and of the power with the help of 4CGM. This allows to characterize an O fed thruster and to compare its functioning with the one expected in case of feed by atmospheric remnants. To this aim, a FD pertaining to atomic oxygen feeding in the pressure region from 1 mTorr to 3 mTorr is presented in Fig. 8. This FD is analogous to the one of Fig. 5 pertaining to atmospheric mixture feeding. The iso-energy curve corresponding to the 1 kW PCC of Fig. 6 is shown here with a thick line. Comparison of Figs. 5 and 8 shows that in case of atmospheric mixture feeding, the ionization is clearly lower than in the atomic oxygen case for similar conditions.

In order to ease the comparison of the FD corresponding to the two different feedings, we provide in Fig. 9, results indicated by thick dashed pink lines joining empty stars, corresponding to pure atomic oxygen feeding, printed on top of the results obtained with atmospheric remnants feeding. For high ionization values (corresponding to high P_{abs} and T_e and low pressure) ionization differences are not exceeding 5%. However, for higher pressure values, around 3 mTorr, ionization are quite different, up to 20% higher in case of atomic oxygen feeding. With increasing pressure, the intrinsic properties of the propellant become more evident.

B. Results of variation of the absorbed power

After investigating the effects of a pressure increase of a few mTorr, we address the effects of varying the absorbed power from a low value of 200 W up to 1.4 kW, first in case of a feed by the 180 km altitude atmospheric remnants mixture, illustrated in Fig. 10. Results will be compared with those obtained by an O_2 feeding shown in Fig. 11. In so doing, we select a typical pressure of 1 mTorr for a feed of 20 sccm. Results follow a power depending version of PCC.

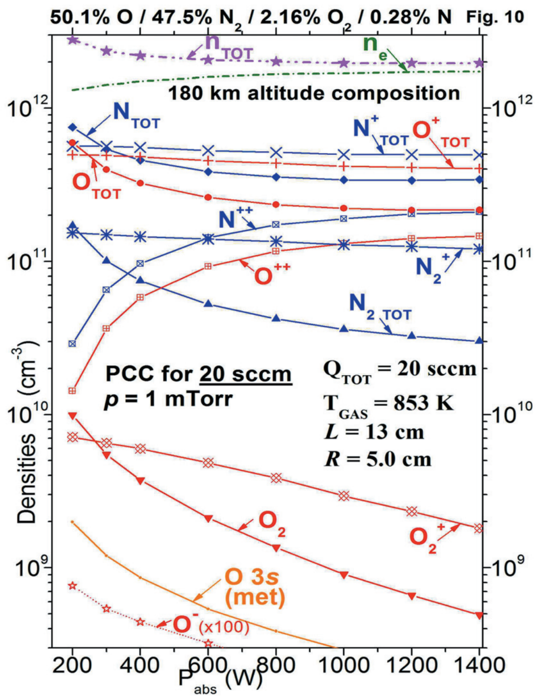

Figure 10. 1 mTorr power depending PCC for atmospheric mixture feeding.

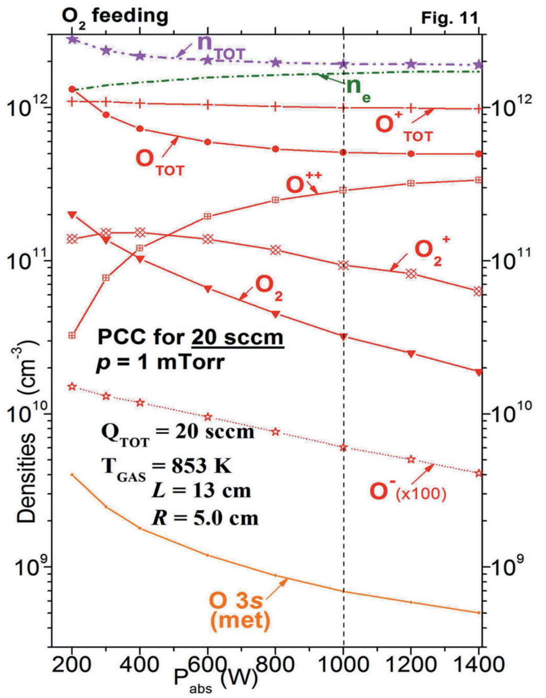

Figure 11. 1 mTorr power depending PCC for O_2 feeding.

PCC of Fig. 10 illustrates that for the chosen conditions important variations appear with P_{abs} changes, especially for low P_{abs} values. N_2 and O_2 densities diminish fast with increasing P_{abs} while presence of N, O atoms is clearly favored in comparison with their corresponding molecules. N density diminishes slower than this of O and remains higher. Also, N_2 presence for 1.4 kW is almost two orders of magnitude higher than this of O_2 , although for 200 W was only about one order. O 3*s* metastable is rather scarce, with an abundance about half than this of O_2 . This illustrates the tendency of an increased molecular N_2 presence in comparison with this of O_2 when absorbed energy increases conformal with what happens in the atmosphere. The atomic ions N^+ and O^+ are the most abundant species, once the absorbed power becomes sufficiently high (about 400 W) for the atoms ionization.

In case of a sole O_2 feeding the situation is quite different, as illustrated in Fig. 11. Part of the absorbed power is spent to dissociate the O_2 molecule. Although O^+ and O^{++} increase considerably as expected, O_2 and O_2^+ presences are much higher than in the atmospheric mixture case, because of the readily available molecule. The total atomic oxygen presence is slightly diminishing when P_{abs} increases and tends to stabilize, as is the case with O^+. The metastable O 3*s* presence is much higher than this calculated for the atmospheric mixture, especially for high P_{abs} . Presence of O^- remains low and diminishes with P_{abs} as was the case for the mixture feed, but for O_2 feed is more than an order of magnitude higher. The vertical line at 1 kW refers to the same conditions with those of Fig. 6 in case of 1 mTorr pressure, showing that O_2 feeding leads in this case to much higher O_2 and O_2^+ populations with similar atomic O presence.

IV. Characterization of ground based experiments for ABET

Various types of ABET prototypes have been considered lately, following an increasing effort of air breathing technology development[13]. Overall theoretical feasibility of RAM-type EP (RAM-EP) has been studied previously by an *ad hoc* ESA interdisciplinary team under the responsibility of J. Gonzalez del Amo and D. Di Cara, as part of the Concurrent Design Facility (CDF)[15]. This study included also an overview of the required technology development for ABET. Recent on-ground experimental devices of interest to ABET are often using N_2 and/or air feed as is the case with Helicon Hall Thruster (HHT)[16], low power radio frequency Helicon Plasma Thrusters (HPT) fed e.g. by argon[17] or laser detonation hyperthermal beam sources[18] addressing atomic oxygen feed. Besides oxygen and/or nitrogen feed, which are the most abundant constituents in LEO environment, propulsion and carrier gases are used to increase O / N speed, typically Ar. The latter, being an inert gas, absorbs electric power mainly for excitation and ionization by electronic collisions, set aside atomic collisions within various species. It has been conjectured lately[19] that O_2 / Ar mixtures may conveniently simulate LEO environment. We consider here characterization of a typical ABIE device producing an hyperthermal atomic O beam when fed by a 30 : 70 [O_2] : [Ar] mixture, as was the case with one of the mixtures addressed in the experiment of Yokota *et al.*[19].

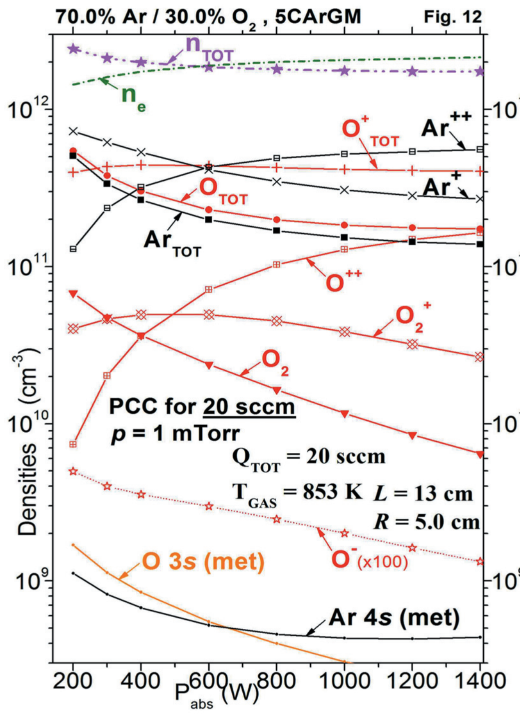

Figure 12. 1 mTorr power depending PCC for 30 : 70 [O_2] : [Ar] feeding.

These authors claim that such a mixture feed simulates sufficiently well LEO conditions. Adding Ar as a fifth component to our 4CGM model, we obtained an adequate global model, 5CArGM, which in principle allows for characterization of such an experiment. Typical results obtained by 5CArGM are presented in Fig. 12. The latter shows an absorbed power depending PCC diagram obtained for a 30 : 70 [O_2] : [Ar] mixture feed of 20 sccm, the rest of the conditions remaining those of the previous Section III. We see in Fig. 12 that atomic O and Ar species have almost the same populations for all absorbed power investigated and especially for lower P_{abs} . Comparing with 4CGM results shown in Fig. 10 we see that O population of 5CArGM is quite similar to this of O in 4CGM in case of atmospheric remnants feeding. Thus, the simulation proposed in the aforementioned experiment[19] is fully justified according to our GM results. As expected, consistent populations of O 3*s* and Ar 4*s* metastable species are shown at the bottom of Fig. 12. These allow for OES diagnostics, even if molecular species also contribute considerably to the spectrum. Using the 5CArGM model version we obtained detailed information meant to implement the one obtained by experimental Time of Flight (TOF) results[19], justifying the use of the O_2 / Ar mixture. Detailed atomic structure of the plasma species is incorporated in 4CGM and 5CArGM allowing for OES diagnostics[20] through comparison of obtained theoretical spectra with experimental ones.

V. Conclusion

Characterization of air breathing electric propulsion devices was investigated on the basis of the adequate 4CGM and 5CArGM models. 4CGM model was able to predict the expected composition of the ABET plasmas described in various PCC diagrams and to define the concomitant ionization in various conditions of low pressure, from which the thrust can be directly inferred. The obtained FDs describe the ABET functioning and give the values pertaining to various conditions of pressure and of absorbed power. Atomic and molecular oxygen feeds were also addressed, allowing for comparison of thruster functioning in various propellants cases. It is shown that feed by atomic oxygen (concomitant to O beam use) is quite different to this by atmospheric remnants four components. Moreover, use of 5CArGM model justified the choice of a 30 : 70 [O_2] : [Ar] mixture feed of ABIE in a recent experiment[19].

Acknowledgments

K. Katsonis and Ch. Berenguer gratefully acknowledge financial support by ESA ESTEC/TEC-MPE.

References

[1]Di Cara, D., Gonzalez del Amo, J., Santovincenzo, A., Carnicero Dominguez, B., Arcioni, M., Caldwell, A., and Roma, I., *RAM Electric Propulsion for Low Earth Orbit Operation: an ESA Study*, IEPC-2007-**162**, IEPC Conference, Florence, Italy, 2007

[2]Katsonis, K., and Berenguer, Ch., *Properties of the Atmospheric Mixtures Prevailing Around 200 km Altitude in Conditions of Low Absorbed Power and Pressure*, 6th ESA Int. Workshop on Rad. of High Temp. in Atm. Entry, St Andrews, UK, November 2014

[3]Katsonis, K., Berenguer, Ch., Gonzalez del Amo, J., and Stavrinidis, C., *Atmospheric Remnants in the Low Earth Orbit Region around 200 km Altitude*, CASE 2015 Conference, Suzhu, China, October 2015, in preparation

[4]ISO/DIS 14222, *Space Environment (natural and artificial) – Earth upper atmosphere*, ISO, Geneva, Switzerland, 2011

[5]Berenguer, Ch., and Katsonis, K., *Plasma Reactors and Plasma Thrusters Modeling by Ar Complete Global Models*, Int. J. Aerospace Eng., vol. **2012**, Article ID 740869, 2012

[6]Katsonis, K., and Berenguer, Ch., *Global Modeling of N_2O Discharges: Helicon Plasma Thruster Application*, Int. J. Aerospace Eng., vol. **2013**, Article ID 467503, 2013

[7]Berenguer, Ch., and Katsonis, K., *Global Modeling of CO_2 Discharges with Aerospace Applications*, Advances in Aerospace Engineering, vol. **2014**, Article ID 847097, 2014

[8]Diamant, K. D., *A 2-Stage Cylindrical Hall Thruster for Air Breathing Electric Propulsion*, 46th AIAA/ASME/SAE/ASEE Joint Propulsion Conference & Exhibit, AIAA 2010-**6522**, Nashville, TN, USA, July 2010

[9]Katsonis, K., Berenguer, Ch., Kaminska, A., and Dudeck, M., *Argon 4s and 4p excited states atomic data applied in ARCJET modeling*, IJAE, vol. **2011**, Article ID 896836, 2011

[10]Katsonis, K., and Berenguer, Ch., *Global Modeling of N_2O Discharges: Rate Coefficients and Comparison with ICP and Glow Discharges Results*, Int. J. Aerospace Eng., vol. **2013**, Article ID 737463, 2013

[11]Katsonis, K., and Berenguer, Ch., *Global Modeling of N_2O, Air and N_2 Discharges and Applications*, Lambert Academic Publishing, Germany, 2013

[12]Katsonis, K., and Berenguer, Ch., *A set of Functioning Diagrams and Plasma Component Compositions for Air Breathing Thrusters Modeling and Diagnostics*, Tech. Report DEDALOS DE-2014-01, Thessaloniki, Greece, July 2014

[13]Katsonis, K., and Berenguer, Ch., *Preliminary design report particle generator*, Technical Note TN-2 for ESA / ESTEC Project No. IPL-PTM/PA/st/541.2014, "Assessment of a neutral particle generator", Report DE-2015-02, Thessaloniki, Greece, March 2015

[14]Katsonis, K., and Berenguer, Ch., *Atmospheric conditions and neutral particles beam flow field specification*, Technical Note TN-1 for ESA / ESTEC Project No. IPL-PTM/PA/st/541.2014, "Assessment of a neutral particle generator", Report DE-2015-01, Thessaloniki, Greece, January 2015

[15]CDF Study Report, Concurrent Design Facility CDF-55(A), RAM-EP Study Report, January 2007

[16]Shabshelowitz, A., *Study of RF Plasma Technology Applied to Air-Breathing Electric Propulsion*, PhD Thesis, University of Michigan, MI, 2013

[17]Pavarin, D., Lucca Fabris, A., Trezzolani, A., Manente, M., Faenza, M., Ferri, F., Selmo, A, Katsonis, K., and Berenguer, Ch., *Low Power RF Plasma Thruster Experimental Characterization*, 48th AIAA Conference, AIAA 2012-**4191**, Atlanta, GE, USA, July-August 2012

[18]Yoneda, S., Tanaka, K., Nomura, S., Matsui, M., Yamagiwa, Y., Komurasaki, and K., Arakawa, Y., *Generation of High Speed Atomic Oxygen Flows by a Laser Driven Plasma Wind Tunnel*, 2011-**r-60p**, 28th International Symposium on Space Technology and Science, Okinawa, 2011

[19]Yokota, K., Watanabe, D., Ohira, J., and Tagawa, M., *Multiple-composition Hyperthermal Atomic Beams Formed by a Laser-induced Plasma for Planetary Environmental Studies*, Phys. Scr. T**161** 014035, 2014

[20]Stavrinidis, C., Gonzalez del Amo, J., Berenguer, Ch., and Katsonis, K., *Diagnostics of Air-Breathing Electric Thrusters*, CASE 2015 Conference, Suzhu, China, October 2015, in preparation